Proceedings of the 2003 IEEE
International Conference on Robotics & Automation
Taipei, Taiwan, September 14-19, 2003

Pushing Manipulation by Humanoid considering Two-Kinds of ZMPs

Kensuke Harada, Shuuji Kajita, Kenji Kaneko, and Hirohisa Hirukawa

Intelligent Systems Institute
National Institute of Advanced Industrial Science and Technology(AIST)
1-1-1 Umezono, Tsukuba 305-8568, JAPAN

Abstract

This paper discusses the pushing manipulation of an object by a humanoid robot. For such a pushing task, we show that there are two kinds of ZMPs, i.e., the conventional "Zero Moment Point (ZMP)" considering all sources of the force/moment acting in the foot supporting area, and the "Generalized Zero Moment Point (GZMP)" which is an generalization of ZMP for a humanoid robot whose hands do not contact with an object. We first obtain the stable region of the GZMP on the floor. Moreover, since the difference between these two ZMPs corresponds to the magnitude of contact force applied by the hands, we propose the pushing manipulation by a humanoid robot by modifying the desired ZMP trajectory for a humanoid. The effectiveness of the proposed method is confirmed by simulation results.

1 Introduction

Since the kinematical structure of a humanoid robot is similar to that of a human, a humanoid robot is expected to work instead of a human in the same environment. Previously, the research of humanoid robot has mainly focused on the hardware design and the realization of some basic motions such as walking and balancing. However, to accomplish the required tasks under such an environment, it should be considered that a humanoid robot manipulates an object cooperating two arms with two legs.

Fig.1 shows a situation where a humanoid robot manipulates a relatively large object. For such a manipulation task, it becomes difficult for a humanoid robot to handle the object by once picking it up. This is because, if a humanoid robot picks up a large object, the robot will easily lose the stability and fall down. Rather, it becomes effective for a humanoid robot to push the object on the floor, and move it to the desired position/orientation. Based on this consideration, we focus on the pushing manipulation of an object by a humanoid in this paper.

Now let us focus on the ZMP(Zero Moment Point) [9] during the pushing manipulation. The ZMP is defined to be a point on the ground at which the tangential component of the moment generated by the ground reaction force/moment becomes zero. If the ZMP is included inside of the convex hull of the foot supporting area, the robot will keep the stability. As shown in Fig.1(a), if the contact force applied by the hands is small, the robot will easily keep the ZMP inside of the supporting area. Then, if the contact force is applied more strongly as shown in Fig.1(b), the ZMP will shift further from the object. To keep the ZMP inside of the convex hull of the foot supporting area, the position of the feet should also shift further from the object. This situation associates the human pushing task where a human leans on the object to push it with strong pushing force. Moreover, since the hands contact with an object, the robot will not always fall down even if the ZMP is on the edge of the foot supporting area. Thus, to perform the pushing manipulation by a humanoid stably, we have to take into account the following things:

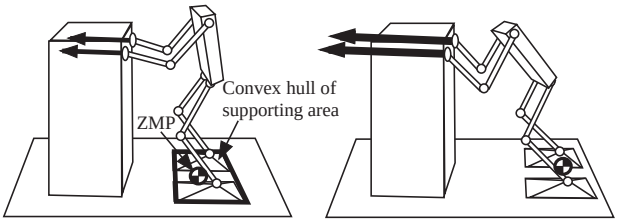

(a) Manipulation with small pushing force

(b) Manipulation with large pushing force

Fig. 1: Pushing Manipulation by a Humanoid Robot

(1)The ZMP during the pushing manipulation depends on the contact force applied by the hands, and

(2)We need to generalize the conventional ZMP to define the stability of the pushing manipulation.

As for (2), we propose two kinds of ZMPs where one is the conventional Zero Moment Point, and the other is the Generalized Zero Moment Point(GZMP) which is an generalization of ZMP for a humanoid robot whose hands do not contact with an object. We will obtain the area of the GZMP on the floor where a humanoid under pushing can keep the stability. As for (1), we show that the difference between these two ZMPs corresponds to the contact force applied by the hands. By

considering the difference between two ZMPs, we construct the controller for the pushing manipulation to be performed stably. Lastly, to show the effectiveness of our idea, some simulation results will be shown.

2 Relevant Works

Inaba et al.[1] constructed small-sized humanoid robots by using the remote-brained approach. Hirai et al.[2] and Kagami et al.[3] constructed human-sized humanoid robots and realized some basic motions. Inoue et al.[4] organized the HRP (Humanoid Robotics Project). Yamane et al.[5] proposed the concept of the dynamics filter for generating the motion of a humanoid robot. Inoue et al.[6] discussed the posture of a humanoid robot maximizing the manipulability index. Kajita et al. discussed the 2D[7] and 3D[8] walking pattern generation of biped robots.

As for the stability index of a biped/quadruped robot, Vukobratovic et al.[9] first proposed the concept of the ZMP(Zero Moment Point). Yoneda et al.[11] proposed another criterion of "Tumble Stability Criterion" for integrated locomotion and manipulation systems. Goswami[10] proposed the FRI(Foot Rotation Indicator). Kitagawa et al.[12] proposed the Enhanced ZMP for the stand-up-motion of a humanoid.

As for the pushing manipulation, Mason et al.[14], Lynch[15], and Harada et al.[16] researched the mechanics of the pushed object. However, there has been no research on the pushing manipulation by a humanoid robot.

3 Two ZMPs

3.1 Formulation

Fig. 2 shows the model of a humanoid pushing an object used in this paper. Σ_R and Σ_i denote the reference coordinate and the coordinate frame fixed to the i-th ($i = 1, \cdots, n$) link of the robot, respectively. $\boldsymbol{p}_{Hj}(= [x_{Hj}\ y_{Hj}\ z_{Hj}]^T)$, and $\boldsymbol{p}_i(= [x_i\ y_i\ z_i]^T)$ denote the position vector of the contact point between the j-th hand and the object, and the origin of Σ_i, respectively. m_i, I_i, and $\boldsymbol{\omega}_i$ denote the mass, the inertia tensor and the angular velocity vector, respectively, of the link i. $\boldsymbol{p}_G(= [x_G\ y_G\ z_G]^T)$ denotes the vector of the center of gravity of the robot defined by $\boldsymbol{p}_G = \sum_{i=1}^n m_i \boldsymbol{p}_i / \sum_{i=1}^n m_i$. $\boldsymbol{p}_Z(= [x_Z\ y_Z\ z_Z]^T)$ and $\boldsymbol{p}_E(= [x_E\ y_E\ z_E]^T)$ denote the position of the zero moment point and the generalized zero moment point, respectively, defined in the following. $\boldsymbol{f}_Z$ and $\boldsymbol{\tau}_Z$ denote the ground reaction force/torque at the ZMP , and $\boldsymbol{f}_E$ and $\boldsymbol{\tau}_E$ denote the reaction force/torque at the GZMP. We assume that the hands apply pushing force onto the object in the horizontal direction; $\boldsymbol{f}_{Hj} = [f_{xj}\ f_{yj}\ 0]^T$.

We now define two kinds of ZMPs existing in the pushing manipulation of a humanoid robot. First, we redefine the conventional definition of ZMP as follows:

Definition 1 (Zero Moment Point)
The zero moment point (ZMP) is the point on the ground at which the moment $\boldsymbol{\tau}_Z = [\tau_{Zx}\ \tau_{Zy}\ \tau_{Zz}]^T$ generated by the reaction force and the reaction moment satisfies $\tau_{Zx} = \tau_{Zy} = 0$, where the reaction force and moment is generated by the inertial force, the gravity force, and the hand reaction force.

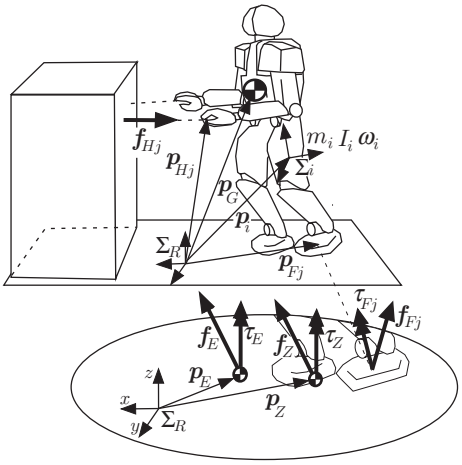

Fig. 2: Model of the System

Since all sources of the reaction force/moment acting in the convex hull of the foot supporting area is considered, this definition becomes equivalent to the conventional definition of ZMP(Fig. 1)[9]. The ground reaction moment at the ZMP is given by

$$\begin{aligned}\boldsymbol{\tau}_Z &= \dot{\boldsymbol{L}}_G + M(\boldsymbol{p}_G - \boldsymbol{p}_Z) \times (\ddot{\boldsymbol{p}}_G - \boldsymbol{g}) \\ &\quad + \sum_{j=1}^{2} (\boldsymbol{p}_{Hj} - \boldsymbol{p}_Z) \times \boldsymbol{f}_{Hj}, \end{aligned} \tag{1}$$

where $M = \sum_{i=1}^n m_i$ and $\boldsymbol{g} = [0\ 0\ -g]^T$, and $\boldsymbol{L}_G(= [L_{Gx}\ L_{Gy}\ L_{Gz}]^T)$ denotes the angular momentum about the center of gravity defined by $\boldsymbol{L}_G = \sum_{i=1}^n (\boldsymbol{p}_i - \boldsymbol{p}_G) \times (m_i \dot{\boldsymbol{p}}_i) + \boldsymbol{I}_i \boldsymbol{\omega}_i$. Substituting $\tau_{Zx} = \tau_{Zy} = 0$ into eq.(1) and solving with respect to $\boldsymbol{p}_Z$, the position of the ZMP can be obtained as

$$\begin{aligned} x_Z &= \frac{-\dot{L}_{Gy} + M x_G(\ddot{z}_G + g) - M(z_G - z_Z)\ddot{x}_G}{M(\ddot{z}_G + g)} \\ &\quad - \sum_{j=1}^{2} \frac{(z_{Hj} - z_Z) f_{xj}}{M(\ddot{z}_G + g)}, \end{aligned} \tag{2}$$

$$\begin{aligned} y_Z &= \frac{\dot{L}_{Gx} + M y_G(\dot{z}_G + g) - M(z_G - z_Z)\ddot{y}_G}{M(\ddot{z}_G + g)} \\ &\quad - \sum_{j=1}^{2} \frac{(z_{Hj} - z_Z) f_{yj}}{M(\ddot{z}_G + g)}. \end{aligned} \tag{3}$$

Here, since the hands apply the contact force onto the object, we can consider the case where the contact forces balance even if the ZMP is on the edge of the convex hull of the foot supporting area. In such a case, the robot will not lose the stability. Then, for the

purpose of generalizing the ZMP to the tasks where a humanoid robot applies the pushing force onto the object, we define the following ZMP:

Definition 2 (Generalized Zero Moment Point)
The generalized zero moment point (GZMP) is the point on the floor at which the moment $\boldsymbol{\tau}_E = [\tau_{Ex}\ \tau_{Ey}\ \tau_{Ez}]^T$ *generated by the reaction force and the reaction moment satisfies* $\tau_{Ex} = \tau_{Ey} = 0$*, where the reaction force and moment is generated by the inertial force and the gravity force.*

In the GZMP, the hand force is not considered in the definition. The reaction torque corresponding to this definition of the GZMP is given by

$$\boldsymbol{\tau}_E = \dot{\boldsymbol{L}}_G + M(\boldsymbol{p}_G - \boldsymbol{p}_E) \times (\ddot{\boldsymbol{p}}_G - \boldsymbol{g}). \quad (4)$$

Substituting $\tau_{Ex} = \tau_{Ey} = 0$ into eq.(4) and solving with respect to $\boldsymbol{p}_E$, the position of the GZMP can be obtained as

$$x_E = \frac{-\dot{L}_{Gy} + Mx_G(\ddot{z}_G + g) - M(z_G - z_E)\ddot{x}_G}{M(\ddot{z}_G + g)}, \quad (5)$$

$$y_E = \frac{\dot{L}_{Gx} + My_G(\ddot{z}_G + g) - M(z_G - z_E)\ddot{y}_G}{M(\ddot{z}_G + g)}. \quad (6)$$

Eqs.(5) and (6) are same as the definition of the ZMP for a humanoid robot whose hands do not contact with an object. Since eqs.(5) and (6) are independent of the pushing force, the robot will lose the stability and fall down if the GZMP is on the edge of the defined area in the following.

3.2 Stable Area

We consider obtaining the stable area of the GZMP on the ground. First, we newly define the point $\tilde{\boldsymbol{p}}_G (= [\tilde{x}_G\ \tilde{y}_G\ \tilde{z}_G]^T)$ and consider the change of coordinates between $\boldsymbol{p}_G$ and $\tilde{\boldsymbol{p}}_G$ as

$$\begin{aligned} -\dot{L}_{Gy}/M + x_G(\ddot{z}_G + g) - (z_G - z_E)\ddot{x}_G & \\ = \tilde{x}_G(\dddot{\tilde{z}}_G + g) - (\tilde{z}_G - z_E)\dddot{\tilde{x}}_G & \quad (7) \\ \dot{L}_{Gx}/M + y_G(\ddot{z}_G + g) - (z_G - z_E)\ddot{y}_G & \\ = \tilde{y}_G(\dddot{\tilde{z}}_G + g) - (\tilde{z}_G - z_E)\dddot{\tilde{y}}_G & \quad (8) \\ \tilde{z}_G = z_G & \quad (9) \end{aligned}$$

By using this change of coordinates, eqs.(5) and (6) become same as those of the inverted pendulum

$$x_E = \frac{\tilde{x}_G(\dddot{\tilde{z}}_G + g) - (\tilde{z}_G - z_E)\dddot{\tilde{x}}_G}{\dddot{\tilde{z}}_G + g} \quad (10)$$

$$y_E = \frac{\tilde{y}_G(\dddot{\tilde{z}}_G + g) - (\tilde{z}_G - z_E)\dddot{\tilde{y}}_G}{\dddot{\tilde{z}}_G + g} \quad (11)$$

As shown in Fig.3(a), the GZMP assumed on the virtual floor can be projected on the real ground by using the following theorem:

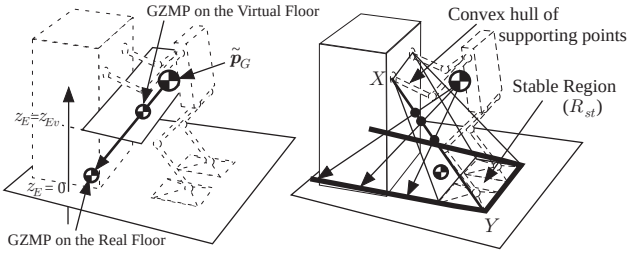

(a) Generalized Zero Moment Point (GZMP)
(b) Stable Region of GZMP

Fig. 3: The Generalized Zero Moment Point

Proposition 1 (Projection of GZMP)
Draw a line including both of $\tilde{\boldsymbol{p}}_G (z_E = z_G)$ *and the GZMP on the virtual floor. The intersection of the line and the ground corresponds to the GZMP on the real ground.*

Proof *In eqs.(10) and (11),* $x_E = \tilde{x}_G$ *and* $y_E = \tilde{y}_G$ *are satisfied when* $z_E = \tilde{z}_G$*. Moreover, since eqs.(10) and (11) are linear equations with respect to* $\boldsymbol{p}_E$*, we confirm the theorem is correct.*

For a humanoid whose hands do not contact with an object to walk stably, the ZMP should be included in the convex hull of the foot supporting area. Also, for a humanoid pushing an object, we consider the convex hull of the supporting points as shown in Fig.3(b). While there are many edges included in the convex hull, we extract the edge of the convex hull where a robot will fall down by the moment around the edge. If the convex hull can rotate around the edge, the following inequality should be satisfied:

$$\boldsymbol{d}^{(XY)} \Delta\theta > 0 \quad (12)$$

where

$$\boldsymbol{d}^{(XY)} = \begin{bmatrix} \{(\boldsymbol{p}_1 - \boldsymbol{p}_{\rm rot}) \times \boldsymbol{n}_1\}^T \\ \vdots \\ \{(\boldsymbol{p}_L - \boldsymbol{p}_{\rm rot}) \times \boldsymbol{n}_L\}^T \end{bmatrix} \frac{\boldsymbol{p}_X - \boldsymbol{p}_Y}{\| \boldsymbol{p}_X - \boldsymbol{p}_Y \|},$$

$$\boldsymbol{p}_{\rm rot} = \boldsymbol{p}_X + (1-t)\boldsymbol{p}_Y \quad (0 \le t \le 1),$$

$\boldsymbol{p}_X$, $\boldsymbol{p}_Y$, and $\boldsymbol{p}_l$ $(l = 1, \cdots, L)$ denote the position vectors of the vertices of the convex hull, $\boldsymbol{n}_l$ $(l = 1, \cdots, L)$ denote the unit normal vector of the surface contacting with the vertex, and t denotes an arbitrary scalar. For given vertices $\boldsymbol{p}_X$ and $\boldsymbol{p}_Y$, if ineq.(12) is satisfied, the convex hull can rotate around the edge including $\boldsymbol{p}_X$ and $\boldsymbol{p}_Y$.

For the motion of a humanoid which can be approximated by an inverted pendulum[7, 8], the reaction torque $\boldsymbol{\tau}_E$ normal to the ground around the GZMP becomes small and can be neglected. In such a case, the moment around the edge can be obtained from the relationship between the position of the GZMP and the line defined in the following theorem.

Theorem 1 (Stable Region of GZMP)
Approximate the motion of the humanoid robot by a

inverted pendulum. Draw a line including both of $\tilde{\boldsymbol{p}}_G$ and the extended line of the edge of the convex hull satisfying ineq.(12). The intersection of the line and ground forms the edge of the stable area of the GZMP.

Here, we note that Kitagawa et al.[12] proposed the Enhanced ZMP. Different from [12], since we consider the GZMP on the ground, we do not need to consider multiple candidate of supporting planes. Also, as shown in the next section, the difference between two ZMPs corresponds to the magnitude of the pushing force. By considering the difference, we can construct the pushing controller. It is our future work extending our method to several cases where the hands slips on the surface of the object, and the humanoid pulls the object etc. An example of the stable area is shown in the appendix.

4 Relationship of Contact Force

Subtracting eqs.(5) and (6) from eqs.(2) and (3), respectively, yields

$$x_E - x_Z = \sum_{j=1}^{2} \frac{(z_{Hj} - z_Z) f_{xj}}{M(\ddot{z}_G + g)}, \tag{13}$$

$$y_E - y_Z = \sum_{j=1}^{2} \frac{(z_{Hj} - z_Z) f_{yj}}{M(\ddot{z}_G + g)}. \tag{14}$$

Eqs.(13) and (14) denote that the difference between the ZMP and the GZMP corresponds to the magnitude of the contact force applied by the hands. Here, since the equations of the GZMP shown in (5) and (6) are same as the equations for a humanoid robot whose hands do not contact with the object, we can obtain the desired motion of a humanoid robot whose hands contact with an object from eqs.(13) and (14). As shown in Fig.4, the desired motion of a humanoid robot whose hands contact with an object can be obtained from the desired motion of a humanoid robot without contacting the object by shifting the position of the desired ZMP by

$$\Delta x = \sum_{j=1}^{2} \frac{(z_{Hj} - z_Z) f_{xj}}{M(\ddot{z}_G + g)}, \tag{15}$$

$$\Delta y = \sum_{j=1}^{2} \frac{(z_{Hj} - z_Z) f_{yj}}{M(\ddot{z}_G + g)}. \tag{16}$$

To plan the desired motion of the pushing task for a humanoid robot, since it is difficult to predict the amount of pushing force in advance of the actual motion, we consider setting Δx and Δy constant. In such a case, with keeping the contact between the sole and the ground, a humanoid robot can support the pushing force within the range of

$$\frac{Mg(\Delta x - l_{af})}{z_{H1} - z_Z} \leq \sum_{j=1}^{2} f_{xj} \leq \frac{Mg(\Delta x + l_{ab})}{z_{H1} - z_Z} \tag{17}$$

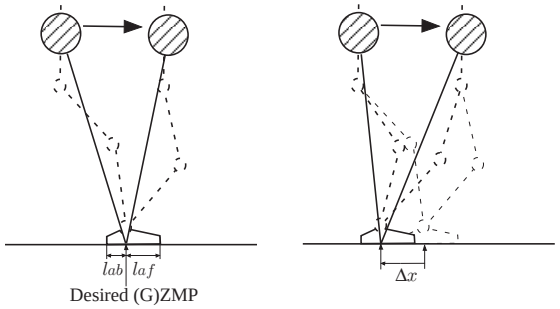

(a) Walking Pattern for a robot whose hands do not contact with an object (b) Modification of the desired ZMP

Fig. 4: Modification of the ZMP position

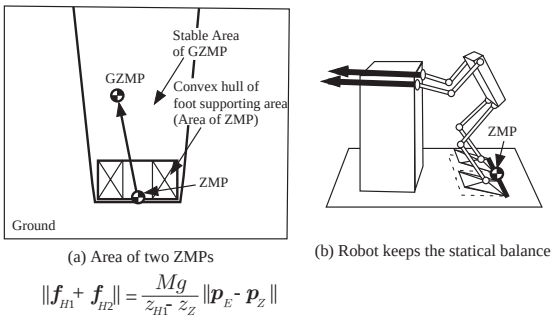

(a) Area of two ZMPs (b) Robot keeps the statical balance

Fig. 5: Relationship between ZMP and GZMP

in the x direction when $z_{H1} \cong z_{H2}$ and $\ddot{z}_G \cong 0$, where l_{ab} and l_{af} denote the length from the desired ZMP to the heel and the length from the desired ZMP to the toe, respectively(Fig.4). We note that if eq.(17) is satisfied, we confirm that the ZMP is included in the convex hull of the foot supporting area. Even if the ZMP is on the edge of the foot supporting area, the robot will not always fall down if the robot is applying the pushing force onto the object(Fig.5). When the ZMP is in the heel, the robot will fall down if the pushing force becomes zero and the GZMP is also in the heel.

5 Controller

The overview of the controller for the pushing manipulation is shown in Fig.6. We assume that the dynamically balanced walking pattern based on the linear inverted pendulum mode[7, 8] is given as a series of the joint trajectory and the desired ZMP trajectory. To support the pushing force, the desired ZMP is modified by Δx. We also implement the stabilizing controller to compensate the error caused in the position of the ZMP as well as the inclination of the body.

6 Simulation

We performed a simulation of pushing manipulation by using the simulation software OpenHRP[17, 18] which is developed in the Humanoid Robotics Project[4]. As a model of humanoid, we used

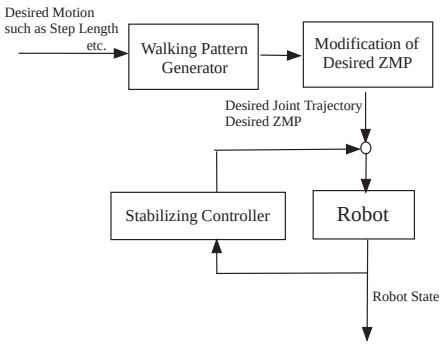

Fig. 6: Overview of the Controller

the physical parameters of HRP-2 prototype(HRP-2P)[19]. HRP-2P is a humanoid whose height and the weight are $H = 1.54$[m] and $M = 58$[kg], respectively. As an object to be pushed we used a box with $M_O = 4$[kg]. The friction coefficient between the object and the floor is set as $\mu = 0.5$. A series of the simulation result is shown in Figs. 7 and 8. In Fig.7, Δx is set as $\Delta x = 0.025$[m], and the humanoid robot can push the object with keeping the dynamical balance. On the other hand, when $\Delta x = 0$, the robot falls down backward.

7 Conclusions

In this paper, we discussed the pushing manipulation by a humanoid robot. Among two kinds of ZMPs proposed in this paper, we have obtained the stable region of GZMP considering the contact points between the hands and the object. By shifting the desired ZMP trajectory based on the difference between the position of the ZMP and the GZMP, we proposed the pushing controller for a humanoid robot. In the simulation, the weight of the object was relatively low. To deal with a heavy object with significant friction, a humanoid robot has to walk in according to the velocity of the object. The pushing manipulation of a heavy object with significant friction is considered to be our future research topic. A concrete analysis of the GZMP is also considered to be our future research topic.

Finally, we would like to express our sincere gratitude for Dr. Kazuhito Yokoi, Dr. Fumio Kanehiro, and Mr. Kiyoshi Fujiwara who are the members of the humanoid robotics group in AIST for their helpful discussions.

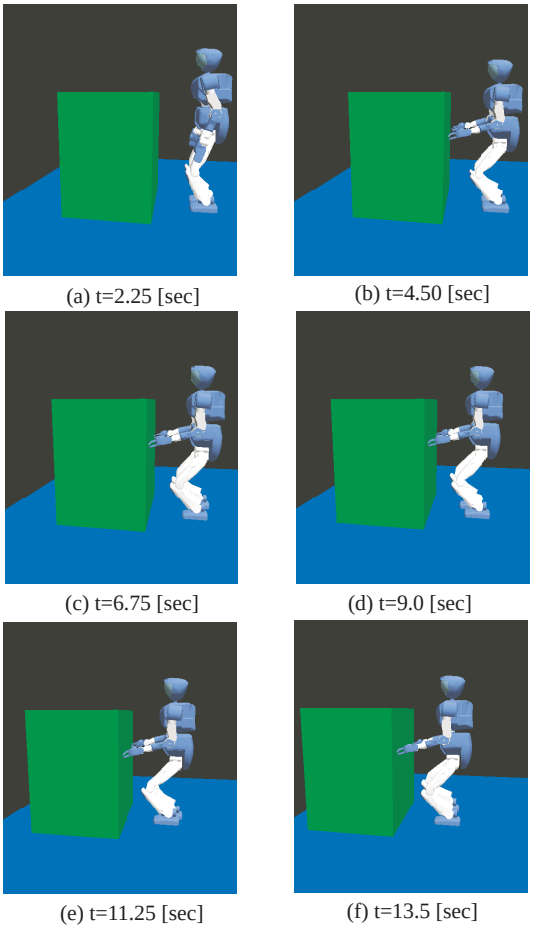

Fig. 7: Simulation Result ($\Delta x = 0.025$)

References

[1] M. Inaba, S. Kagami, F. Kanehiro, Y. Hoshino, and H. Inoue: "A Platform for Robotics Research Based on the Remote-Brained Robot Approach", Int. J. Robotics Res., vol.19, no.10, pp. 933-954, 2000.

[2] K. Hirai, M. Hirose, Y. Haikawa, T. Takenaka: "The Development of Honda Humanoid Robot", Proc. of IEEE Int. Conf. on Robotics and Automation, pp. 1321-1326, 1998.

[3] S. Kagami, A. Konno, R. Kageyama, M. Inaba, H. Inoue: "Development of a Humanoid H4 with Soft and Distributed Tactile Sensor Skin", Experimental Robotics VI, Lecture Notes in Control and Information Sciences 250, pp. 499–507, Springer, 1999.

[4] H. Inoue et al.: "HRP: Humanoid Robotics Project of MITI", Proc. of the First IEEE-RAS Int. Conf. on Humanoid Robots, 2000.

[5] K. Yamane and Y. Nakamura: "Dynamics Filter–Concept and Implementation of On-Line Motion Generator for Human Figures–", Proc. of IEEE Int. Conf. on Robotics and Automation, pp. 688-694, 2000.

[6] K. Inoue, H. Yoshida, T. Arai, and Y. Mae: "Mobile Manipulation of Humanoids –Real-Time Control Based on Manipulability and Stability–", Proc. of IEEE Int. Conf. on Robotics and Automation, pp. 2217-2222, 2000.

[7] S. Kajita, T. Yamaura, and A. Kobayashi: "Dynamic Walking Control of a Biped Robot Along a Potential Energy Conserving Orbit", IEEE Trans. Robot. and Automat., vol. 8, no. 4, pp. 431-438, 1992.

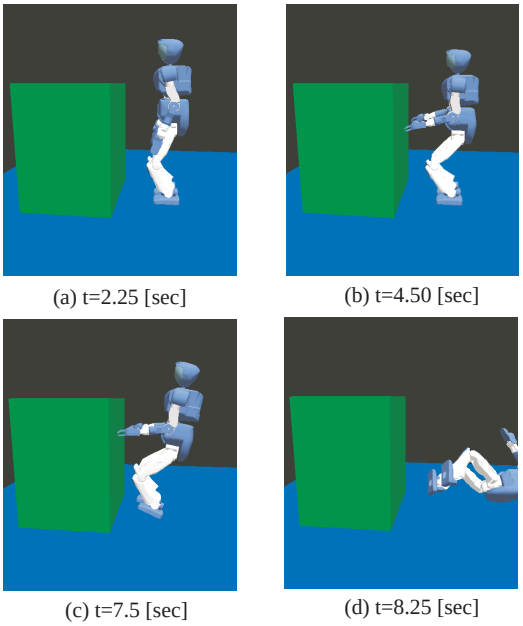

Fig. 8: Simulation Result ($\Delta x = 0.0$)

[8] S. Kajita, O. Matsumoto, and M. Saigo: "Real-time 3D Walking Pattern Generation for a Biped Robot with Telescopic Legs", Proc. of IEEE Int. Conf. on Robotics and Automation, pp. 2299-2036, 2001.

[9] M. Vukobratovic and J. Stepanenko: "On the Stability of Anthropomorphic Systems", Mathematical Biosciences, vol. 15, pp. 1-37, 1972.

[10] A. Goswami: "Postural Stability of Biped Robots and the Foot Rotation Indicator(FRI) Point", Int. J. of Robotics Res., vol. 19, no. 6, pp. 523-533, 1999.

[11] K. Yoneda S. Hirose: "Tumble Stability Criterion of lntegrated Locomotion and Manipulation", Proc. of IEEE/RSJ Int. Conf. on Intelligent Robots and Systems, pp.870-876, 1996.

[12] T. Kitagawa, K. Nagasaka, K. Nishiwaki, M. Inaba, and H. Inoue: "Generation of Stand-up-motion with Genetic Algorithm for a Humanoid", Proc. of the 17th Annual Conf. of RSJ, pp. 1191-1192, 1999.

[13] K. Nagasaka, M. Inaba, and H. Inoue: "Stabilization of Dynamic Walk on a Humanoid using Torso Position Compliance Control", Proc. of the 17th Annual Conf. of RSJ, pp. 1193-1194, 1999.

[14] M.T.Mason and J.K Salisbury: "Robot Hands and the Mechanics of Manipulation". MIT Press, Cambiridege MA, 1985.

[15] K.M.Lynch: "The Mechanics of Fine Manipulation by Pushing". Proc. of IEEE Int. Conf. on Robotics and Automation, pp.2269-2276, 1992.

[16] K. Harada, J. Nishiyama, Y. Murakami, and M. Kaneko: "Pushing Multiple Objects using Equivalent Friction Center", Proc. of IEEE Int. Conf. on Robotics and Automation, pp. 2485-2491, 2002.

[17] F. Kanehiro et al.: "Virtual humanoid robot platform to develop controllers of real humanoid robots without porting", Proc. of IEEE/RSJ Int. Conf. on Intelligent Robots and Systems, 2001.

[18] H. Hirukawa et al.: "OpenHRP: Open Architecture Humanoid Robot Platform", Proc. of Int. Symp. on Robotics Research, 2001.

[19] K. Kaneko et al.: "Design of Prototype Humanoid Robotics Platform for HRP", Proc. of IEEE/RSJ Int. Conf. Intelligent Robots and Systems, 2002.

A Example on Stable Area

In this section, we briefly show an example of the stable area outlined in the subsection 3.2. Fig.9 shows an example of convex hull where $\boldsymbol{p}_G = [0\ 0\ 2]^T$, $\ddot{\boldsymbol{p}}_G = [1\ 1\ 0]^T$, and $\dot{\boldsymbol{L}}_G = \mathbf{o}$. By calculating ineq.(12), we can see that the convex hull can rotate around the edges of BC, CD, BE, and DE, and cannot rotate around the edges of AD, AB, AE, and EC. The result of calculation is shown in Table 1. By projecting the edges, we can obtain the stable area of the GZMP as shown in Fig.9(b).

Table 1: Result of calculation

$d^{(EA)}$	$[0.6667\ -0.6667\ -1.3333]^T$
$d^{(EC)}$	$[0.2481\ 1.4884\ -1.2403]^T$
$d^{(EB)}$	$[-0.3123\ -1.8741\ -2.1864]^T$
$d^{(ED)}$	$[0.6963\ 2.4371\ 1.7408]^T$
$d^{(AB)}$	$[-2\ -2\ 1]^T$
$d^{(CD)}$	$[-2\ -2\ -1]^T$
$d^{(AD)}$	$[2\ 2\ -2]^T$
$d^{(BC)}$	$[-2\ -2\ -2]^T$

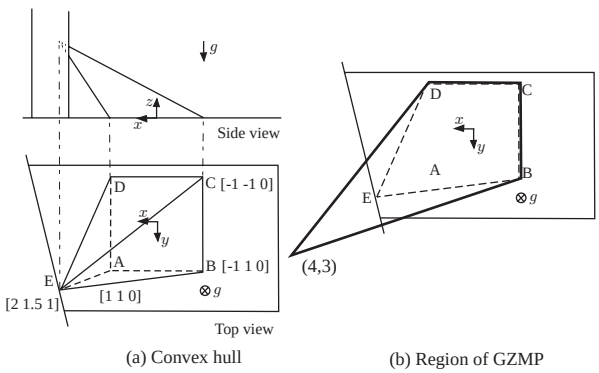

(a) Convex hull (b) Region of GZMP

Fig. 9: Numerical Example